

Collapse of large vapor bubbles

James Tegart and Sam Dominick

Propulsion Section, Martin Marietta Denver Aerospace
P. O. Box 179, Denver, Colorado 80201Abstract

The refilling of propellant tanks while in a low-gravity environment requires that entrapped vapor bubbles be collapsed by increasing the system pressure. Tests were performed to verify the mechanism of collapse for these large vapor bubbles with the thermodynamic conditions, geometry, and boundary conditions being those applicable to propellant storage systems. For these conditions it was found that conduction heat transfer determined the collapse rate, with the specific bubble geometry having a significant influence.

Introduction

The capability of refilling the storage tanks for liquid propulsion systems while a spacecraft is in earth orbit will yield a number of benefits. With refilling, the life of a spacecraft can be extended or a space-based vehicle could be reused for numerous missions. Methods of refilling a propellant tank while in low-gravity are currently being developed. This paper considers one aspect of tank refilling: the collapse of vapor bubbles that may become entrapped within the tank during filling.

Expulsion of liquid propellants from a tank under low-gravity conditions requires some means of ensuring that only liquid will be supplied to the engine. Capillary propellant management devices, using fine-mesh screen to orient liquid and exclude gas are the likely choice for the expulsion system, especially for cryogenic propellant applications. These devices are now being used for propellant expulsion on the Space Shuttle¹ and various communications satellites. In one configuration, the fine-mesh screen is used on channels mounted near the tank wall and encircling the tank. These channels form a flow passage from the bulk liquid, regardless of its orientation, to the tank outlet. Liquid flows through the screen in preference to gas, due to the capillary pressure differential developed at the pores of the screen.

During the filling of the tank, vapor bubbles can be entrapped within the channels of the capillary device if the screen becomes wetted before the vapor can escape. Vapor cannot be permitted to remain within the channels of the device since it could cause dryout of the screen and failure of the ability of the device to expel gas-free liquid. Such vapor bubbles can be eliminated by pressurizing the tank, making the liquid subcooled with respect to the vapor pressure and causing the vapor to condense. Collapse of the vapor bubble must occur within a reasonable length of time (preferably minutes) so that the refilling process can be completed and the subsequent mission for the spacecraft begun.

A survey of the analytical and experimental investigations of bubble collapse can be found in reference 2. Of the work surveyed, that of Florschuetz and Chao³ seems the most comprehensive. It defines the regimes in which inertia, heat transfer, or both mechanisms determine the bubble collapse rate. For the case of heat transfer controlled collapse (of interest here) Florschuetz and Chao consider a solution based on the Plesset-Zwick temperature integral⁴ to be an upper bound for the bubble size versus time curve and their "plane interface" solution to be an "approximate lower limit". However, Prigynakov⁵ obtained a solution that "gives better agreement with experiments" and predicts a faster rate of collapse. Likewise, the analysis of Theofanous² predicts a faster collapse rate than Florschuetz and Chao and "improvements in the agreement are noted" when non-equilibrium effects were considered.

In applying any of the above theories to predict collapse times during tank refilling there are two concerns. One is that the collapse time for bubbles with volumes on the order of 100 cm³ is desired, while the above theories have only been verified with tests of bubbles on the order of 1 cm³. The second concern is that bubbles in contact with the inside walls of the channels will be elongated in shape, while the existing theory is applicable only to spherical bubbles. An analytical and experimental investigation was therefore performed to determine the influence of bubble size and shape on the collapse time.

Analysis

Florschuetz and Chao³ define a dimensionless parameter, B_{eff} , to classify the mode of bubble collapse. For values of B_{eff} less than 0.05 heat transfer controls the collapse while values greater than 10 indicate inertia controls. An intermediate case exists between these values. The parameter is defined as

$$B_{eff} = \gamma^2 \left(\frac{\rho_c \Delta T}{\beta_v L} \right)^2 \frac{\alpha}{r_i} \left(\frac{\rho}{\Delta P} \right)^{1/2} \quad (1)$$

(A list of symbols can be found at the end of this paper.)

Values of B_{eff} were calculated for typical conditions in a propellant tank and the range of conditions planned for the experiments, and it was established that in all cases B_{eff} is much less than 0.05 (on the order of 10⁻⁵), indicating that heat transfer will control the rate of bubble collapse.

The configuration of the bubble within the channel is as shown in Figure 1. Both screen and sheet metal surround the bubble on four sides with a vapor-liquid interface at each end. Under low-g conditions the liquid interface will have curvature, but a flat interface has been assumed here to simplify the analysis. It was assumed that the vapor bubble and liquid are initially in equilibrium and then the system pressure is instantaneously increased by some amount. The increase in pressure increases the saturation temperature of the vapor above the liquid temperature. This change in the thermodynamic condition results in condensation of the vapor and collapse of the bubble.

The change in the volume of the vapor bubble is dependent on the rate at which vapor condenses.

$$dV = \frac{1}{\rho_v} dm \quad (2)$$

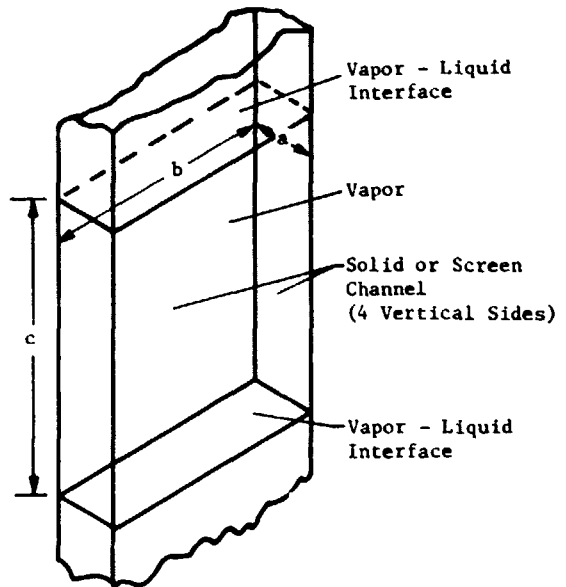


Figure 1. Bubble Geometry

The rate of condensation is dependent upon the rate at which heat is transferred from the vapor to the surrounding liquid.

$$dm = \frac{Q}{L} dt \quad (3)$$

Therefore

$$dV = \frac{1}{\rho_v} \frac{Q}{L} dt \quad (4)$$

The greater saturation temperature causes the vapor to condense on the liquid, creating a liquid film that is at the saturation temperature. Condensation continues based on the rate at which this heat can be conducted into the liquid. Convection heat transfer is negligible since the vapor temperature remains essentially unchanged during collapse. The unsteady heat conduction into a semi-infinite solid is given by ⁶

$$Q = \frac{kA\Delta T}{\sqrt{\pi\alpha t}} \quad (5)$$

The conductivity is that of the liquid only since the contribution of the thin sheet metal and screen has a negligible effect on the heat transfer rate (this assumption will be discussed in more detail later). Then

$$\frac{dV}{A} = \frac{k\Delta T dt}{\rho_v L \sqrt{\pi\alpha t}} \quad (6)$$

which can be reduced to

$$\frac{dV}{A} = \sqrt{\frac{\alpha}{\pi}} Ja \frac{dt}{t} \quad (7)$$

where Ja, the Jacob number, is defined as

$$Ja = \frac{\Delta T_c \rho_l}{L \rho_v} \quad (8)$$

Based on the bubble geometry in Figure 1,

$$dV = ab \, dc \quad (9)$$

and

$$A = 2ab + 2bc + 2ac \quad (10)$$

After integration, the following equation is obtained for the collapse of the bubble from its initial length (c_i) to any final length (c_f).

$$t = \frac{\pi}{4Ja^2\alpha} \left[\frac{ab}{2(a+b)} \ln \frac{(a+b)c_f + ab}{(a+b)c_i + ab} \right]^2 \quad (11)$$

For complete collapse of the bubble c_f equals zero. It was assumed that only the length of the bubble changes as it collapses, but there would be a transition to a spherical bubble when the length c approached the channel thickness, a . Based on the assumptions it would be expected that this equation would be most applicable to the collapse of larger bubbles and be least accurate for the collapse of smaller bubbles and the final stages of collapse of any bubble.

It is interesting to note that if a spherical bubble geometry is used in solving equation (7), then $dV = dr$ and the time for a bubble to completely collapse from an initial radius (r_i) is:

$$t = \frac{\pi r_i^2}{4Ja^2g} \quad (12)$$

This is the same result Florschultz and Chao³ obtained for their plane interface solution. Priskyakov⁵ obtained a similar result except that the coefficient was 16 instead of 4.

For a given bubble volume, equations (11) and (12) were used to calculate bubble collapse times. For larger bubbles the difference in geometry causes the rectangular shaped bubble to collapse about four times as fast as a spherical bubble of the same volume.

Experiments

In order to verify the analytical model presented in the previous section and to investigate the influence of bubble geometry and the channel on bubble collapse, an experimental investigation was performed. The approach was to form a bubble within a channel, pressurize the container in which the channel was installed and monitor the collapse of the bubble. Since a stationary bubble can be formed and confined within the liquid by the channel, a one-g test closely represents the low-g conditions. The mechanism of the bubble collapse, conduction heat transfer, is independent of the g-level and only minor changes in the shape of the vapor bubble would be expected in low-g.

A transparent channel, to permit viewing of the vapor bubble, was fabricated from plastic. It had an inside cross-section of 2.5 cm by 7.6 cm and was 30.5 cm long. One side of the channel (see Figure 2) was a fine mesh screen having a 325 x 2300 (wires per inch in warp and shute directions) mesh, Dutch twill weave and an effective pore diameter of 7 microns. This screen was capable of retaining any size vapor bubble within the channel. The channel was installed vertically within a transparent plastic box (Figure 3).

Freon 11 (CCl₃F) was selected as the test liquid. This Freon has a boiling point of 23.8°C at 1 atm so vapor bubbles could be easily created under ambient conditions. Liquid Freon 11 has the following properties at 20°C: $\rho = 1.49 \text{ gm/cm}^3$, $L = 43.1 \text{ cal/gm}$, $c_p = 0.205 \text{ cal/gm}^\circ\text{C}$ and $\alpha = 2.5 \times 10^{-4} \text{ m}^2/\text{hr}$. The saturation curve is linear, having a slope of 0.32°K per kPa.

The test procedure was to fill the channel and container with liquid so the channel was completely filled and submerged, excluding all air from the channel. While maintaining the container at a higher pressure to inhibit boiling, the channel was vented to form the vapor bubble. If necessary, a vapor generator could be used to aid in forming a bubble of the desired initial size. The size of the bubble was monitored to ensure that the vapor was initially in equilibrium with the liquid. The initial temperature of the liquid, system pressure and bubble length were recorded.

A gaseous nitrogen pressurization system connected to the container was set to give a desired increase in system pressure. The valve that applied the pressure increase to the container had an opening time that was negligible in comparison to the typical collapse times of 1 to 11 seconds. A motion picture camera photographed the bubble collapse. The bubble length versus time was measured using a scale on the channel and the frame rate of the camera. A total of 99 tests were performed, primarily varying the initial bubble length and the amount of pressure increase.

For data correlation, the analytical model was adapted to the specific test conditions. The plastic walls of the channels influenced the modeling of the heat transfer, while the effect of the screen could be neglected. The plastic was 1.3 cm

ORIGINAL PAGE
BLACK AND WHITE PHOTOGRAPH

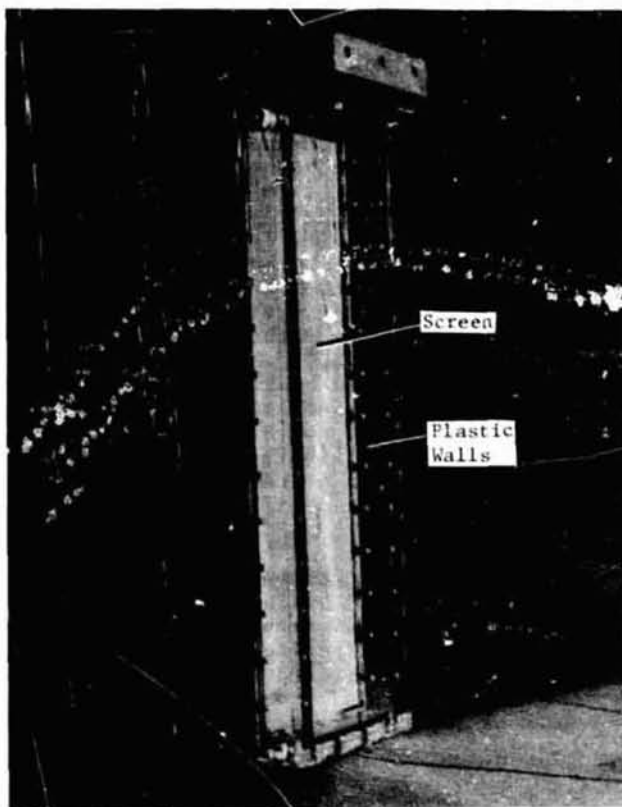


Figure 2. Channel Model

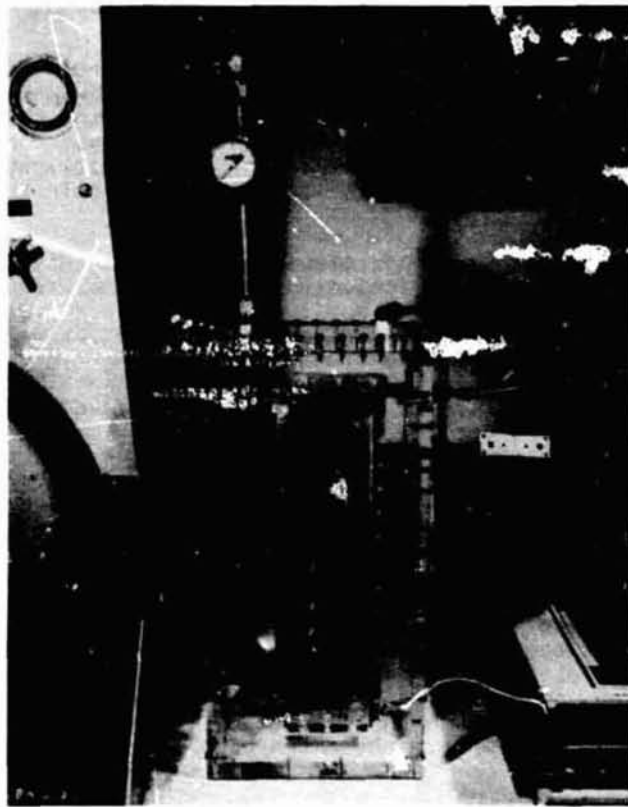


Figure 3. Test Apparatus

thick and had a diffusivity of $4.5 \times 10^{-4} \text{ m}^2/\text{hr}$ (twice the value for the liquid), while the screen was 0.064 mm thick and had a diffusivity of $1.5 \times 10^{-2} \text{ m}^2/\text{hr}$ (stainless steel). The thermal penetration thickness given by⁷

$$\delta_t = \sqrt{4\alpha t} \quad (13)$$

was used to evaluate the relative influence of the materials of the test article. For the vertical plastic walls the heat conduction occurred solely within the plastic so the liquid adjacent to the outside of the channel did not contribute to the heat transfer. The screen quickly reached the temperature of the surrounding liquid due to its thinness and high diffusivity, so its contribution to conduction perpendicular to its surface was negligible. Similarly, heat conduction parallel to the screen was shown to be negligible. Therefore, the heat transfer at the surfaces of the bubble were modeled as follows:

upper surface and 3 vertical sides - unsteady conduction into plastic, and screen surface and liquid surface - unsteady conduction into liquid

Equation (5) with the appropriate values for k and A was used for both cases.

From the film data it was established that the collapse of the bubble occurred as a rise in the liquid surface, changing only the length of the bubble, until small values of bubble length were reached. At bubble lengths less than one centimeter the bubble began to decrease in width and during the last stages of collapse the bubble reached a

spherical shape and then disappeared. The data correlation concentrated on the initial stages of collapse when only the length of the bubble was changing and the major change in volume occurred.

As previously discussed it was established that the screen had a negligible effect on the heat transfer into the liquid. However, another potential influence of the screen is the effect of its flow resistance on the collapse rate. Liquid must flow through the screen, filling the channel as the vapor condenses. An analysis determined that the pressure drop due to flow at the rate established by the bubble collapse had a negligible effect on the pressure of the liquid within the channel.

Preliminary correlations indicated that the bubble collapsed faster than predicted by equation (11) (including the above discussed modifications). Therefore a correlation coefficient, F , was applied to equation (5) for the heat transfer rate, giving a term F^2 in the denominator of equation (11). It was found that the value of F that best correlated the collapse time of the bubbles typically ranged from 1.3 to 2.0. Neither the initial length of the bubble nor the change in system pressure appeared to have any effect on the variation in the value of F . Based on the excellent and more constant correlation obtained for the bubbles having long collapse times, a value of 1.4 for F was selected as giving the best fit. This means that the coefficient in equation (11) is increased to 8, placing the value midway between that of Florschuetz and Chao³ with a coefficient of 4 and Prisyakov⁵ with a coefficient of 16.

Figure 4 is an example of the correlation of a test in which the bubble had a long collapse time. A very close match between the calculated and measured collapse rate was obtained over the latter 10 seconds of the test. During the first 1.5 seconds of the test the bubble collapsed at a slower rate than predicted. This initial difference in the calculated and measured collapse rate becomes more evident in the shorter duration tests shown in Figures 5 and 6. Changing the heat transfer rate (through F) only changed the point at which the curves for the calculated and measured collapse rate intersected and did not improve the match of their slopes.

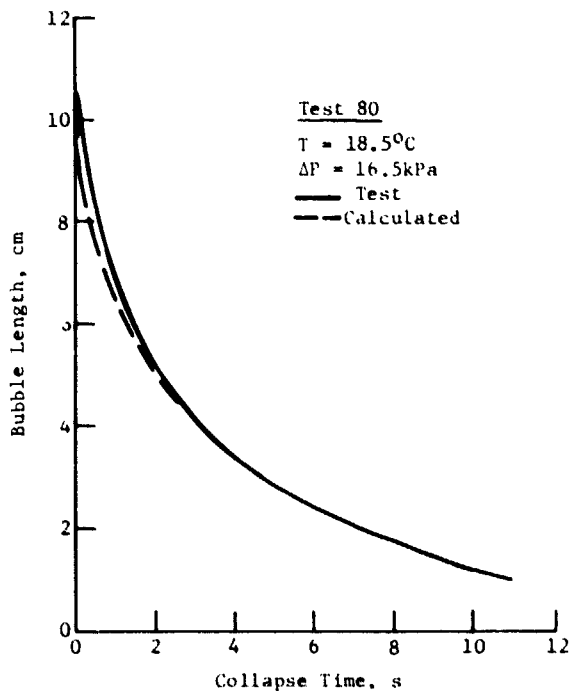


Figure 4. Correlation of Bubble Collapse, Long Collapse Time

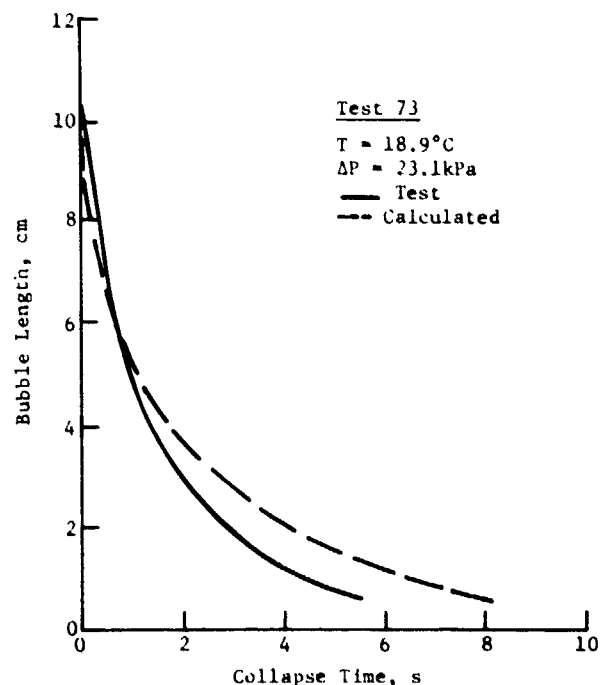


Figure 5. Correlation of Bubble Collapse Intermediate Collapse Time

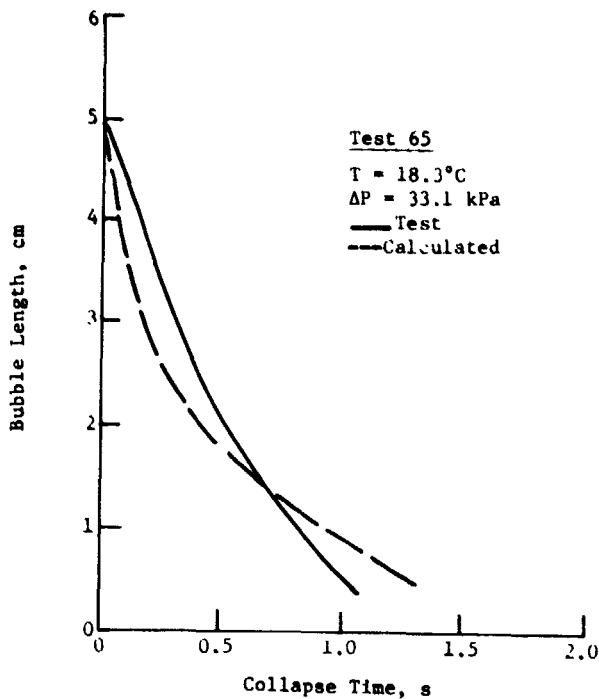


Figure 6. Correlation of Bubble Collapse, Short Collapse Time

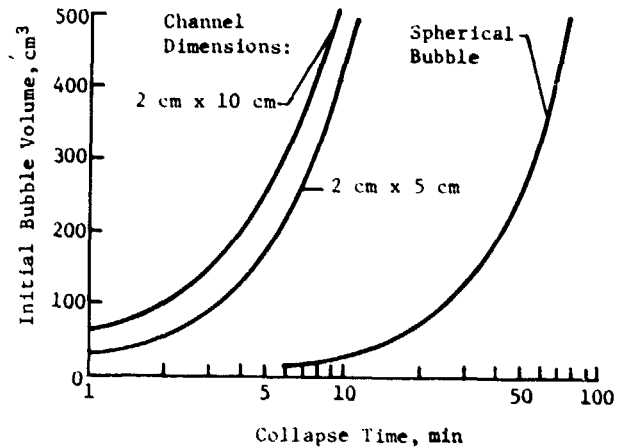


Figure 7. Collapse of Hydrogen Vapor Bubbles, $T = 20.2^\circ\text{K}$, $\Delta P = 50 \text{ kPa}$

Conclusions

An analytical and experimental investigation of the collapse of a large vapor bubble inside of a channel has established that conduction heat transfer is the primary mechanism of collapse for the conditions of interest. It was found that the elongated shape of the bubble decreased the collapse time in comparison to a spherical bubble of the same volume. An analytical model, based on conduction heat transfer to the surrounding liquid, gave excellent correlation of those tests having a longer collapse time (~ 10 seconds).

It appears that there are two stages to the bubble collapse, based on the tests performed here. In the initial stage, lasting about 1.5 seconds, the rate of collapse was less than predicted by the heat transfer model. Apparently the inertia of the liquid, flowing into the channel through the screen to replace the condensed vapor, reduced the initial collapse rate. This effect made the correlation of the shorter duration tests less accurate.

During the later stage of collapse the rate was greater than predicted by the heat transfer model. This deficiency was corrected by the correlation coefficient which resulted in matching of the rates and times of collapse during that stage. This difference is typical of the variation noted in other bubble collapse analyses, as discussed in the introduction. When the collapse time is long, the influence of the initial phase became insignificant and the heat transfer model accurately predicted the collapse time.

A correlation coefficient of 1.4 was selected as giving the best fit to all the data. Based on the data, the following equation will accurately predict the longer collapse times and it will predict too long a time for short collapse periods.

$$t = \frac{\pi}{8Ja^2\alpha} \left[\frac{ab}{2(a+b)} \ln \frac{ab}{(a+b)c_1 + ab} \right]^2 \quad (14)$$

When this equation is used to predict the collapse time of hydrogen vapor bubbles the result shown in Figure 7 is obtained. The saturation curve for hydrogen is non-linear and the change in saturation temperature with pressure becomes small at pressures above 100 kPa. For example, at 100 kPa a 50 kPa change in pressure causes the saturation temperature to change by only 1.5°K. Collapse times of many minutes, or even hours, are possible with hydrogen. Hydrogen presents a "worst-case" in comparison to other propellants for the problem of collapsing entrapped vapor bubbles during tank refill.

In comparison to the collapse time for a spherical bubble (based on Ref. 3), equation (14) yields a collapse time for an equal volume bubble in a channel that is about 10 times less. At these low collapse rates inertia effects should be negligible, so the assumptions applicable to equation (14) are justified for this application and reasonably accurate predictions of the collapse time should be expected.

List of Symbols

A	area
a,b,c	bubble dimensions
B _{eff}	dimensionless group
c _p	specific heat of liquid
F	correlation coefficient
Ja	Jacob number
k	thermal conductivity of liquid
L	heat of vaporization
m	mass
ΔP	difference between system pressure and vapor pressure
Q	rate of heat transfer
r	bubble radius
t	time
ΔT	difference between vapor saturation temperature and liquid temperature
V	volume
α	thermal diffusivity of liquid
ρ	liquid density
ρ _v	vapor density
ρ̄ _v	average vapor density
ψ	temperature difference correction factor (see Ref. 3)
δ _t	thermal penetration thickness

References

- 1 Peterson, R. and Uney, P., Development and Qualification of the Space Shuttle Orbiter Reaction Control System Propellant Tank, AIAA Paper 78-1026, AIAA/SAE 14th Joint Propulsion Conference, Las Vegas, Nevada, July 1978.
- 2 Theofanous, T.G., et al, Nonequilibrium Bubble Collapse: A Theoretical Study, Chemical Engineering Progress Symposium Series, No. 102, Vol. 66, 1970, pp 37-46.
- 3 Florschuetz, L.W. and Chao, B.T., On the Mechanics of Vapor Bubble Collapse, Journal of Heat Transfer, May 1965, pp 209-220.
- 4 Plesset, M.S. and Zwick, S.A., The Growth of Vapor Bubbles in Superheated Liquids, Journal of Applied Physics, Vol. 25, No. 4, April 1954, pp 493-500.
- 5 Prismanyakov, V. F., Condensation of Vapour Bubbles in Liquid, Int. J. Heat Mass Transfer, Vol. 14, 1971, pp 353-356.
- 6 Carslaw, H.S. and Jaeger, J.C., Conduction of Heat in Solids, Oxford at the Clarendon Press, 1959.
- 7 Bird, R.B., Stewart, W.E., and Lightfoot, E.N., Transport Phenomena, John Wiley and Sons, Inc., 1960, p354.